Some geomechanical issues of relevance for energy production

Guido Musso
Politecnico di Torino

IV International workshop
Modern Trends in Geomechanics
Assisi, May 16 -18 2016

Activities into which geomechanics plays a crucial role in the Oil & Gas field

- Design of infrastructures (platform foundations, pipelines, etc..)
- Gas hydrates;
- Fault reactivation – earthquakes;
- CO_2 and Methane sequestration;
- Unconventional hydrocarbons (tar sands, gas shales, etc..);
- Reservoir or well stimulation (e.g. water flooding, hydraulic fracturing);
- Subsidence modelling and forecast;
- Well design (wellbore stability, design of wellbore completions, sand production)

New applications ↑

Traditional applications ↓

Objectives of the talk: improving forecast and modelling of failure at the wellbore scale

Well casings and completion

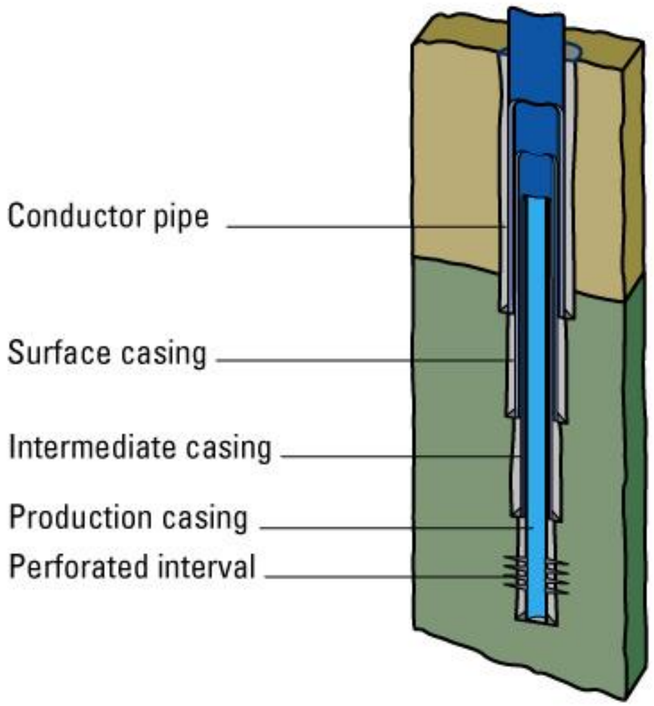

Example of well completion (Schlumberger)

Drilling + completion of one well: tens of millions of USD (say 50 millions)

It depends on geology, off shore / on shore, direction of drilling, completion type

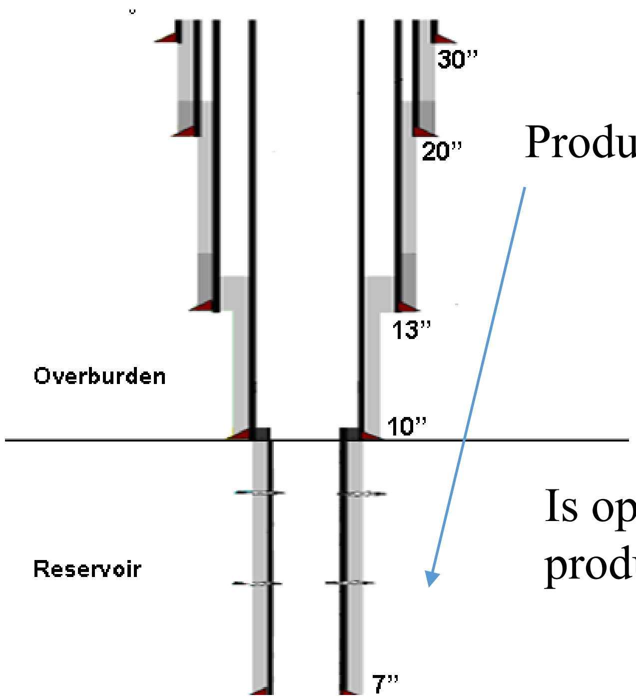

Producing layers: open hole vs cased hole?

Is open hole completion safe along the productive life of the field?

Stress state determination

Critical needs: Characterization of field conditions (saturation, fluid pressure and **stress state**)

Normal

$S_v > S_{Hmax} > S_{Hmin}$

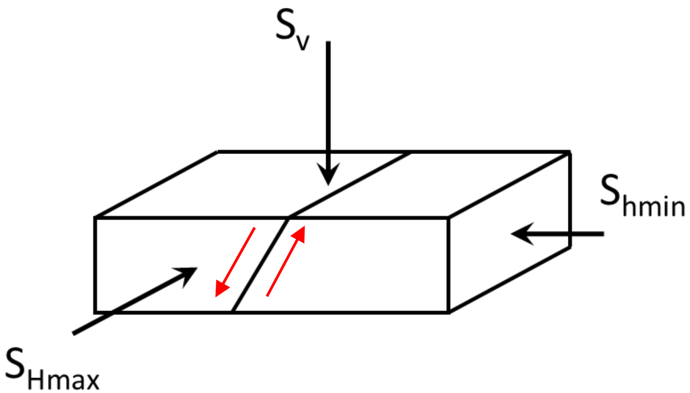

Strike slip

$S_{Hmax} > S_v > S_{Hmin}$

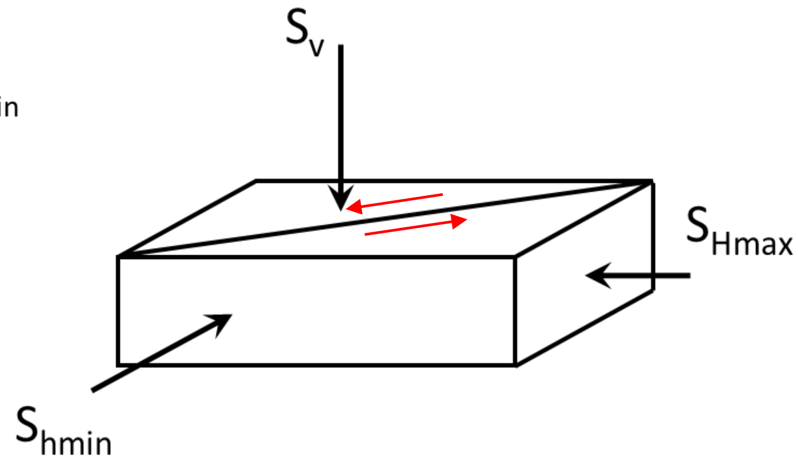

Reverse

$S_{Hmax} > S_{hmin} > S_v$

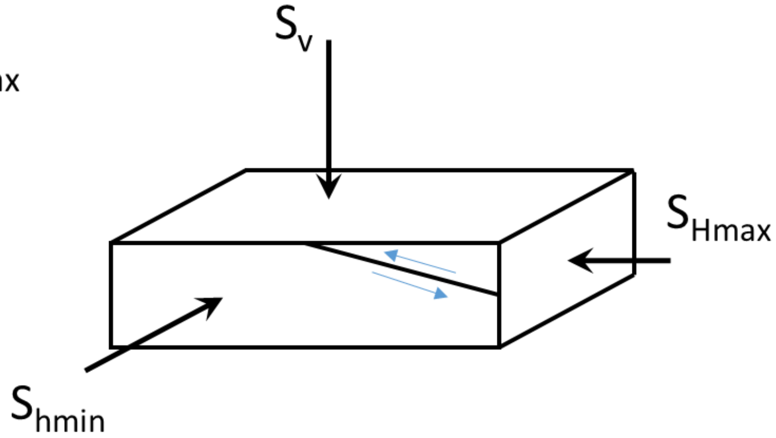

Critical needs:

6 variables :
- 3 principal stress directions (reduced to 2 if the vertical is one of those);
- 3 principal stress magnitude

Can we find a simple way to invert solutions of the stability problem to determine missing values for the far field stress?

Max. shear stress

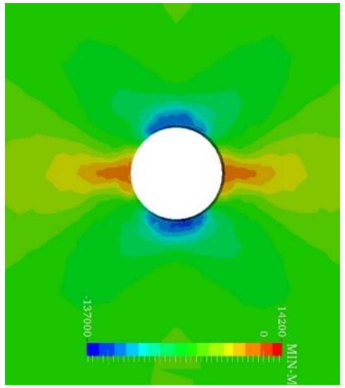

Max. σ_3

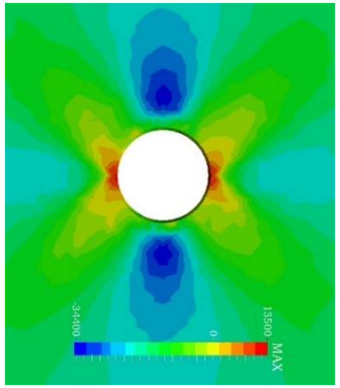

‘cracks’ opening

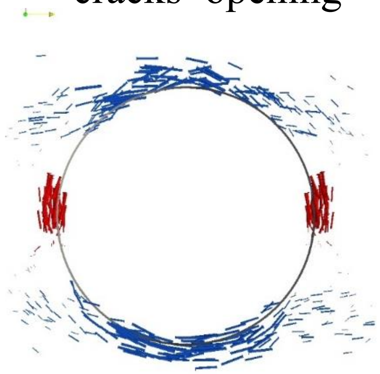

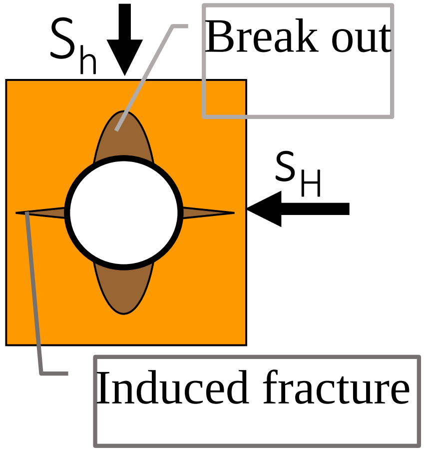

De Bellis et al. (2016), MoM

Stress state determination

Della Vecchia, Pandolfi, Musso & Capasso (2013) An analytical expression for the determination of in situ stress state from borehole data accounting for breakout size – Int. J. Rock Mech. Mining. Sci

→ S_v is the overburden stress: calculated through the density log

$$S_v = \int_0^z \rho(\xi) g \, d\xi$$

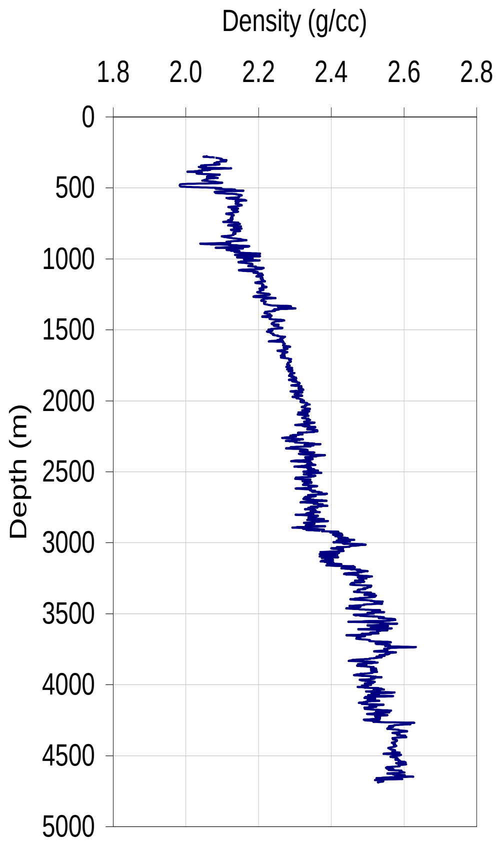

→ Principal directions can be identified through analysis of failures on the well detected through image logs

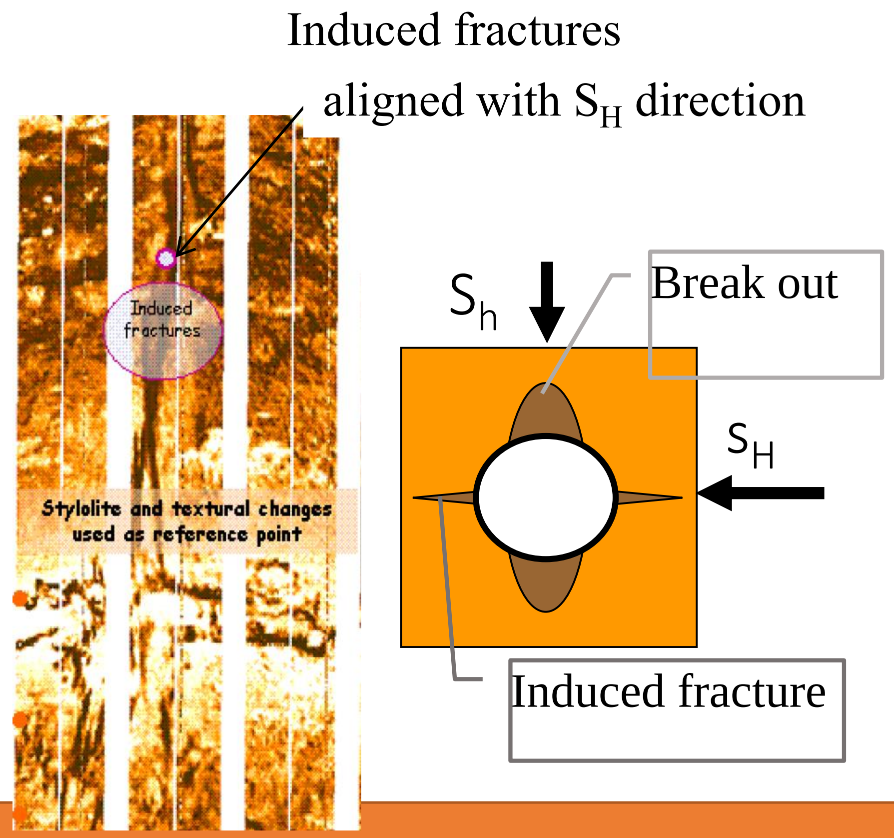

Stress state determination

→ The minimum principal stress S_3, coincident with S_h except for reverse faulting regimes, can be obtained by hydraulic frac test (both magnitude and direction).

→ Pore pressure p_w can be directly measured (sometimes estimated with geophysical logs)

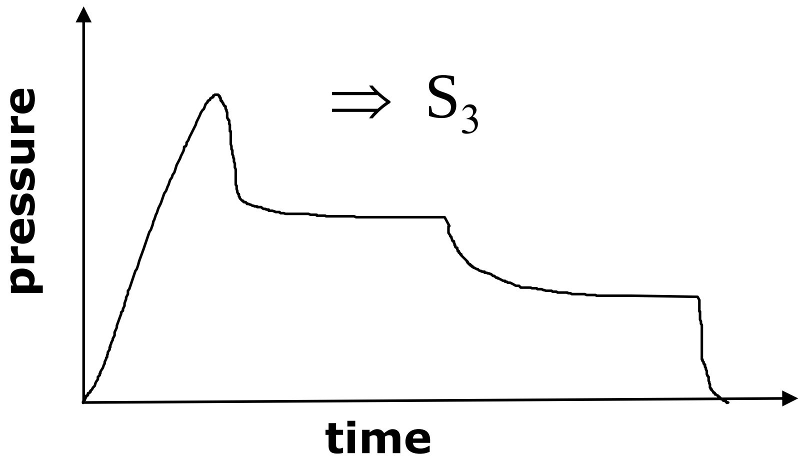

→ Boundaries for S_H deduced from compressive and tensile failures recovered on circular borehole walls as a consequence of excavation

Stress state determination

Circular hole of radius a in a isotropic linear elastic half-space:

→ Plane strain ($\Delta\varepsilon_z$=0)

→ Far-field stresses: S_H e S_h (S_H>S_h)

→ Uniform internal pressure p_i and pore pressure p_w.

→ Net pressure $p_{net} = p_i - p_w$

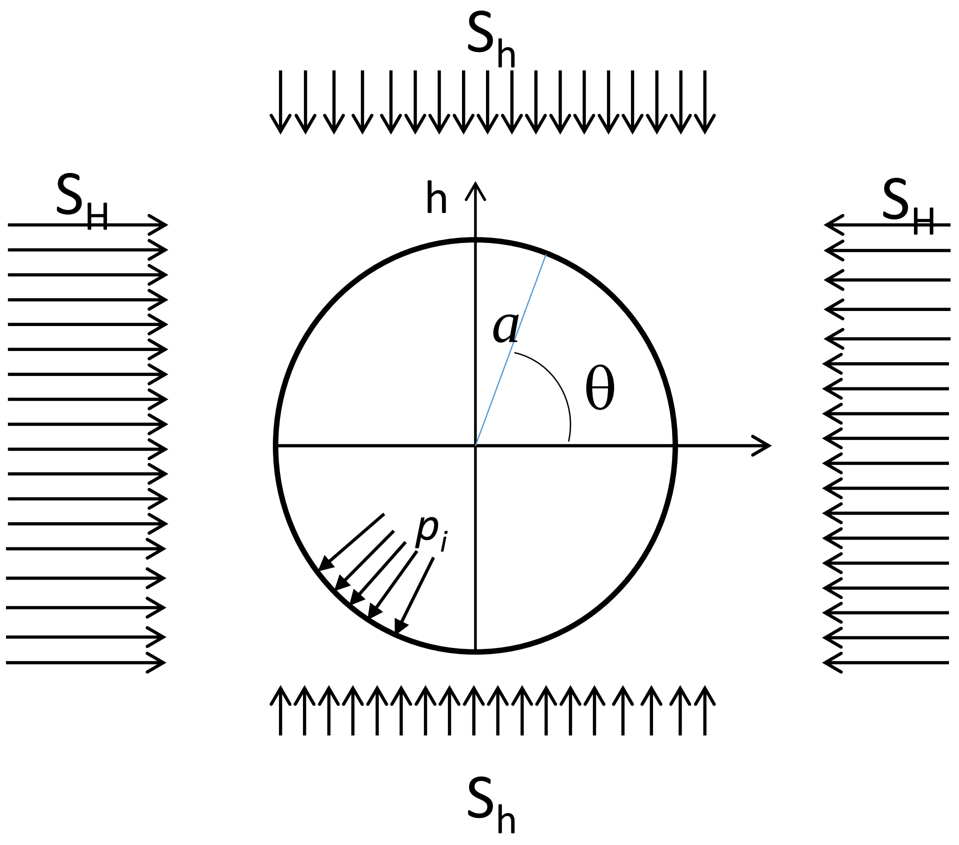

Kirsh solution: perturbation of the stress field due to the hole as a function of S_H and S_h

$$\sigma'_r = \frac{1}{2}(S'_H + S'_h)\left[1 - \left(\frac{a}{r}\right)^2\right] + p_{net}\left(\frac{a}{r}\right)^2 + \frac{1}{2}(S'_H - S'_h)\left[1 - 4\left(\frac{a}{r}\right)^2 + 3\left(\frac{a}{r}\right)^4\right]\cos 2\theta,$$

$$\sigma'_\theta = \frac{1}{2}(S'_H + S'_h)\left[1 + \left(\frac{a}{r}\right)^2\right] - p_{net}\left(\frac{a}{r}\right)^2 - \frac{1}{2}(S'_H - S'_h)\left[1 + 3\left(\frac{a}{r}\right)^4\right]\cos 2\theta,$$

$$\tau_{r\theta} = -\frac{1}{2}(S'_H - S'_h)\left[1 + 2\left(\frac{a}{r}\right)^2 - 3\left(\frac{a}{r}\right)^4\right]\sin 2\theta.$$

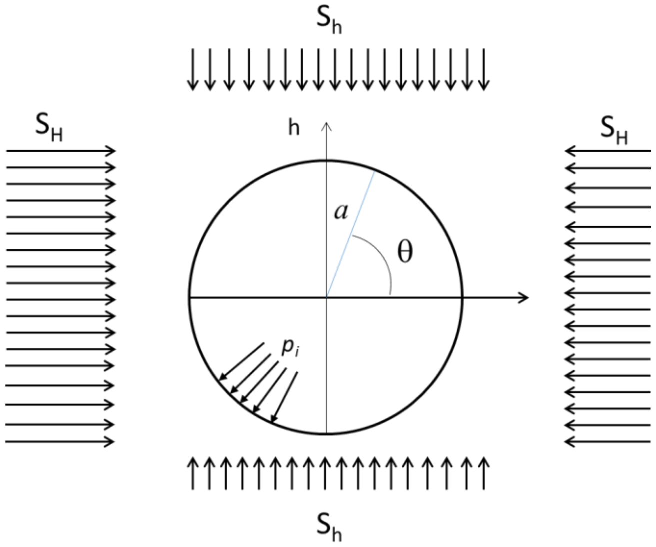

The perturbation vanishes proportionally to $(a\,/\,r)^2$

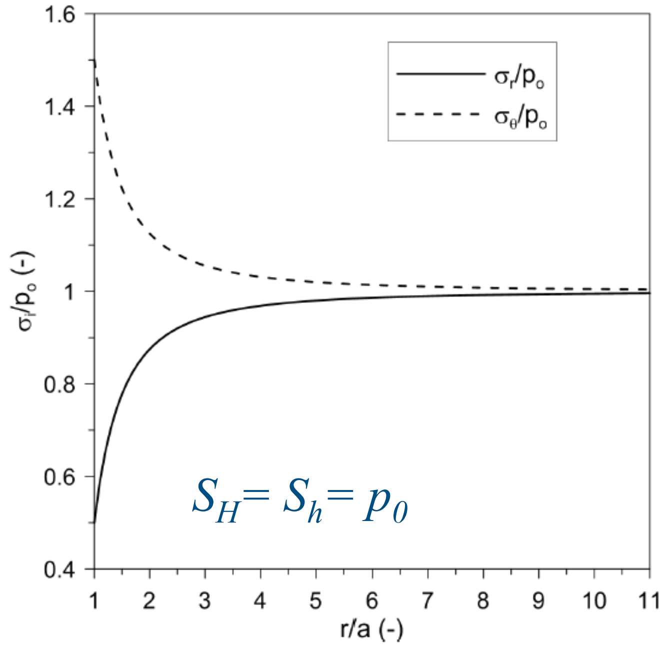

Stress state determination

On borehole wall ($r = a$):

$$\sigma'_\theta(a,\theta) = (S'_H + S'_h) - p_{net} - 2(S'_H - S'_h)\cos 2\theta$$
$$\sigma'_r(a,\theta) = p_{net}$$

→Maximum hoop stress:

$\sigma'_\theta = 3S'_H - S'_h - p_{net}$

(for $\theta=\pi/2$ and $\theta=3/2\pi$)

→ Minimum hoop stress:

$\sigma'_\theta = 3S'_h - S'_H - p_{net}$

(for $\theta=0$ and $\theta=\pi$)

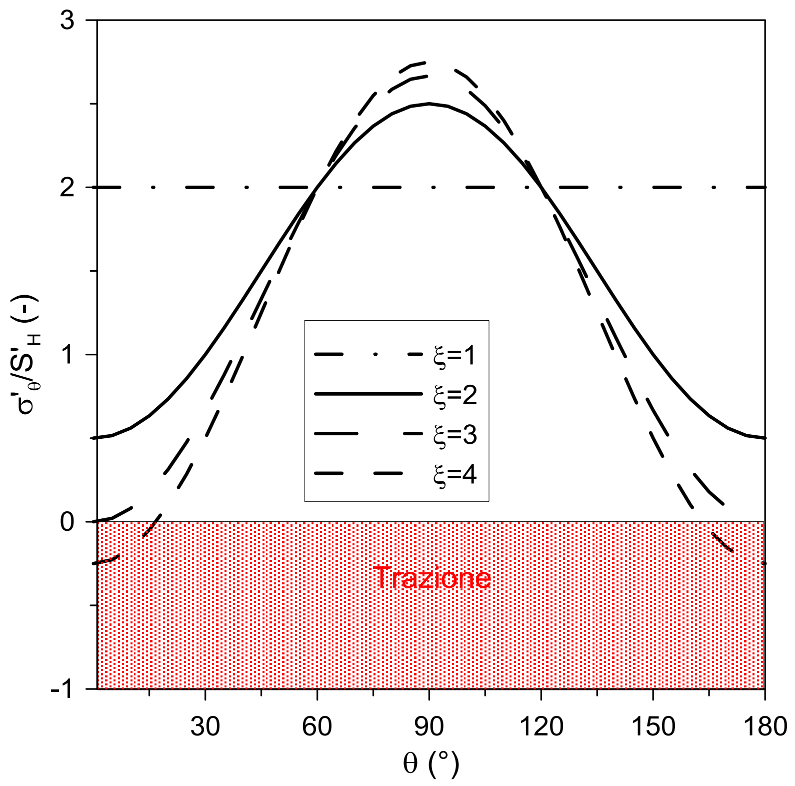

$\xi = S_H/S_h$, $p_{net}=0$

→*Breakout*: compressive failure process that occurs when the maximum hoop stress σ'_θ is such thath the shear resistance of the rock is exceeded.

Stress state determination

If breakout failure occurs (from dipmeters or televiewers) → estimate of a lower bondary for S_H (=S_H^{min}).

for $\theta=\pi/2$

$$\sigma'_\theta = 3S'_H - S'_h - p_{\mathrm{net}},$$
$$\sigma'_z = S'_v + \Delta\sigma'_z,$$
$$\sigma'_r = p_{\mathrm{net}}.$$

Hp. Plane strain excavation process ($\Delta\varepsilon_z = 0$).

$$\Delta\sigma'_z = \nu\left(\Delta\sigma'_r + \Delta\sigma'_\theta\right).$$

Assuming that the material fails:

$$f_C\left(\sigma'_z(S'^{\mathrm{min}}_H), \sigma'_r, \sigma'_\theta(S'^{\mathrm{min}}_H)\right) = f_C(S'^{\mathrm{min}}_H) = 0,$$

→ Suitable failure criterion

If breakout failure does not occur, the methodology allows the estimate of S_H^{max}.

Stress state determination

E.g: Mohr-Coulomb criterion $\sigma_1' = C + N_\phi \sigma_3'$

Minimum principal stress not known a priori

If $\sigma_1' = \sigma_\theta', \quad \sigma_3' = \sigma_r',$

$$S_H'^{\min} = \frac{1}{3}\left[S_h' + (1 + N_\phi)p_{\text{net}} + C\right]$$

If $\sigma_1' = \sigma_\theta', \quad \sigma_3' = \sigma_z'.$

$$S_H'^{\min} = \frac{C + N_\phi S_v' + S_h'(1 - 2\nu N_\phi) + p_{\text{net}}}{3 - 2\nu N_\phi}$$

Stress state determination

- Aim: improve the predictive capability of the methodology taking into account the amplitude of breakout failure.
- Previous solutions (Zoback et al., 1985) are base on the thickness of the spalled area t
- Hp. In situ measured breakout size = size of the yielding zone that would originate in the same conditions in a elastic-perfectly-plastic material

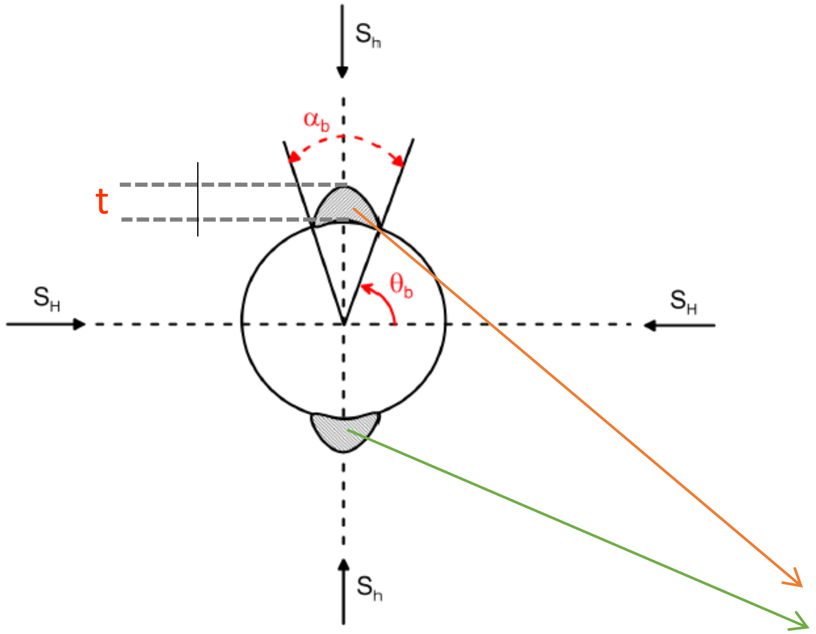

α_b = breakout amplitude

θ_b = azimuth of the radius passing from the extremity of the breakout zone

$$\theta_b = \frac{\pi}{2} - \frac{\alpha_b}{2}$$

Yielded zones

Stress state determination

Principal stresses on the borehole wall for $\theta=\theta_b$ (hp. $\Delta\varepsilon_z = 0$)

$$\sigma'_\theta = S'_H + S'_h - p_{\text{net}} - 2(S'_H - S'_h)\cos 2\theta_b,$$
$$\sigma'_z = S'_v - 2\nu(S'_H - S'_h)\cos 2\theta_b,$$
$$\sigma'_r = p_{\text{net}}.$$

Hp. In $\theta = \theta_b$ the material is prone to yield:

→The elastic solution holds;

→The stress state satisfies the yielding condition;

→An estimate of S'_H is obtained as a function of the amplitude of the breakout zone.

Caution: stress redistribution induced by inelastic deformation is NOT taken into account

Stress state determination

E.g. Mohr-Coulomb criterion $\sigma_1' = C + N_\phi \sigma_3'$

if $\sigma_1' = \sigma_\theta'$, $\sigma_3' = \sigma_r'$,

$$S_H' = \frac{C - S_h'(1 + 2\cos 2\theta_b) + (1 + N_\phi)p_{\text{net}}}{1 - 2\cos 2\theta_b},$$

[mud pressure lower than vertical stress]

if $\sigma_1' = \sigma_\theta'$, $\sigma_3' = \sigma_z'$.

$$S_H' = \frac{C + N_\phi S_v' + S_h'\left[-1 - 2\cos 2\theta_b(1 - \nu N_\phi)\right] + p_{\text{net}}}{1 + 2\cos 2\theta_b(\nu N_\phi - 1)},$$

[mud pressure higher than vertical stress]

θ_b = azimuth of the radius passing from the extremity of the breakout zone

Stress state determination

FEM simulations to validate the analytical approach

$N_\phi = 4.6$ ($\phi' = 40$)

$C = 0$

$\nu = 0.3$

Simulation sequence:

1. Determination of the initial stress state due to S_v and $S_H = S_h$.
2. Modelling of the borehole through the application of the net pressure p_{net} in plane strain conditions.
3. **Increment of S_H** keeping fixed p_{net} and S_h in plane strain conditions

(Steps 1–2: NO plastic strains)

Stage in which plastic strains are anticipated: evaluation of the link between S'_H e θ_b.

Stress state determination

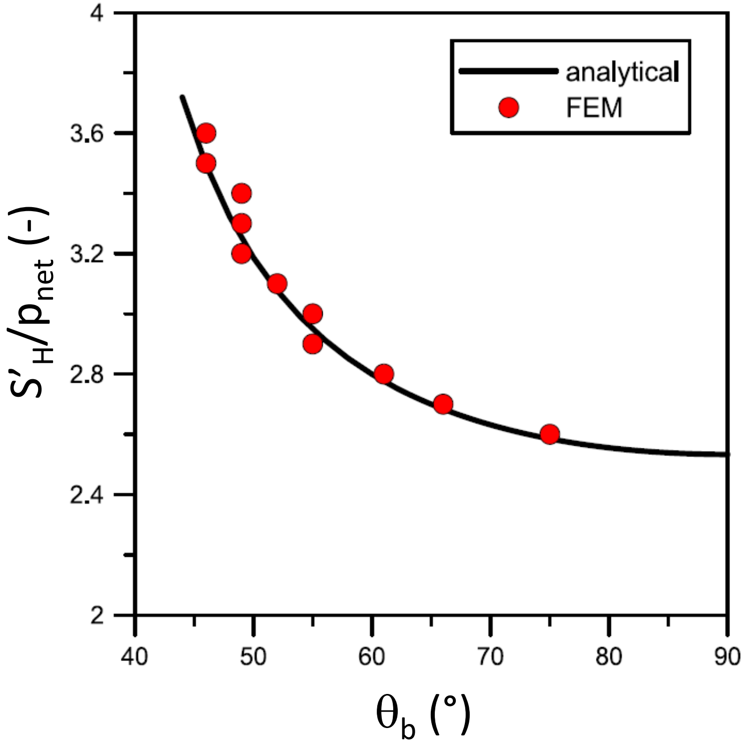

Normal faulting regime
($S_v>S_H>S_h$)
$S'_v/p_{net} = 4$, $S'_h/p_{net} = 2$

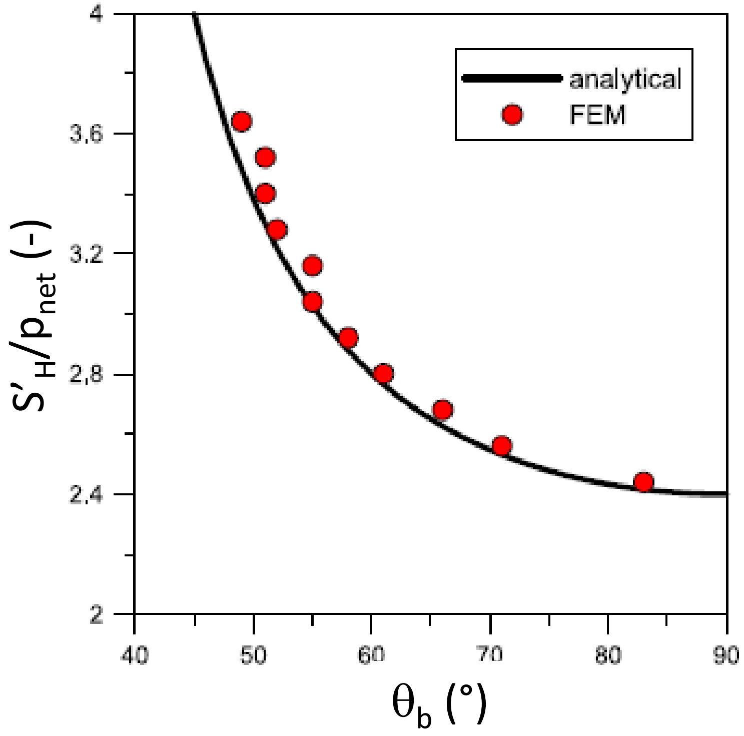

Reverse faulting regime
($S_H>S_h>S_v$)
$S'_v/p_{net} = 1.6$, $S'_h/p_{net} = 2.4$

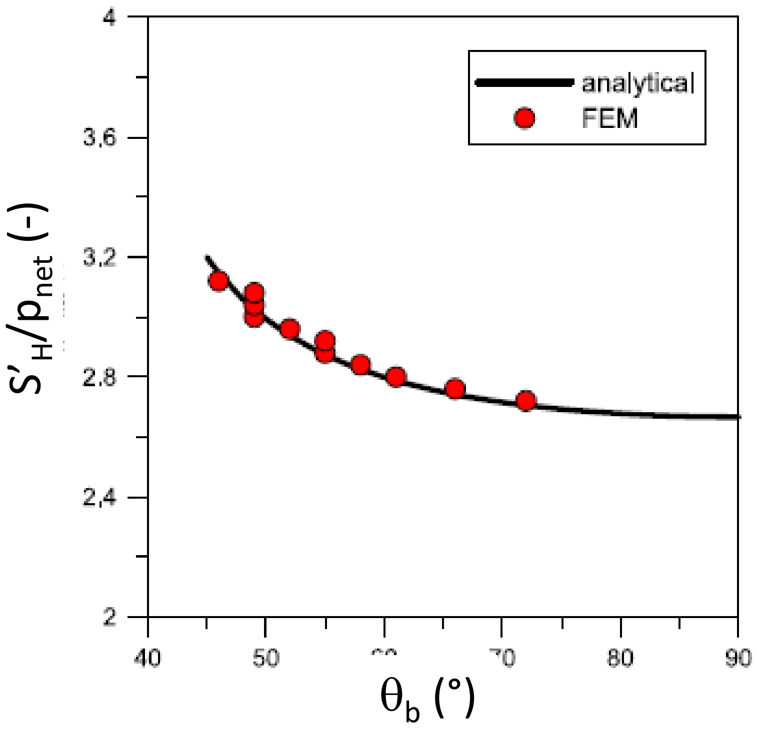

Strike-slip faulting regime
($S_H>S_v>S_h$)
$S'_v/p_{net} = 2$, $S'_h/p_{net} = 1.6$

Stress state determination

Advantages of the present solution with respect to previous ones:

- takes into account the influence of p_{net}
- valid for every faulting regime including the case in which the radial stress is the inter- mediate principal stress (and so it does not contribute to the shear resistance if a Mohr–Coulomb criterion is assumed);
- the information about the deepest radius reached by breakout failure is not needed

Prediction of S'_H/p_{net} as a function of ϕ' for different values of θ_b.

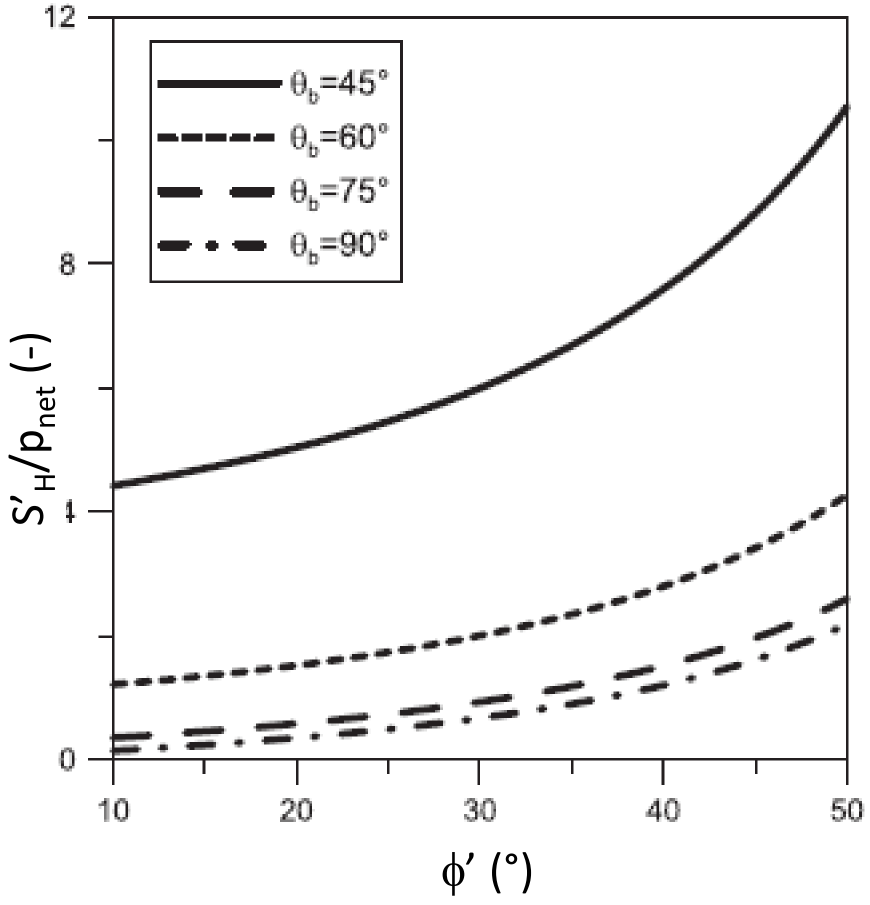

Stress state determination

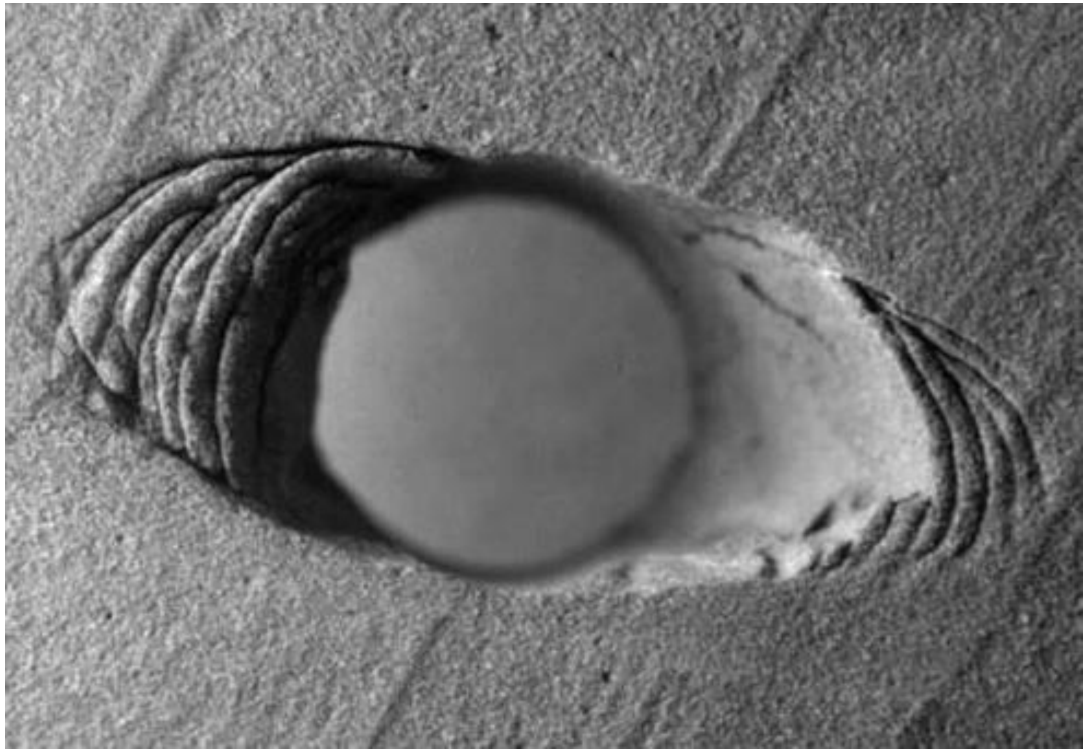

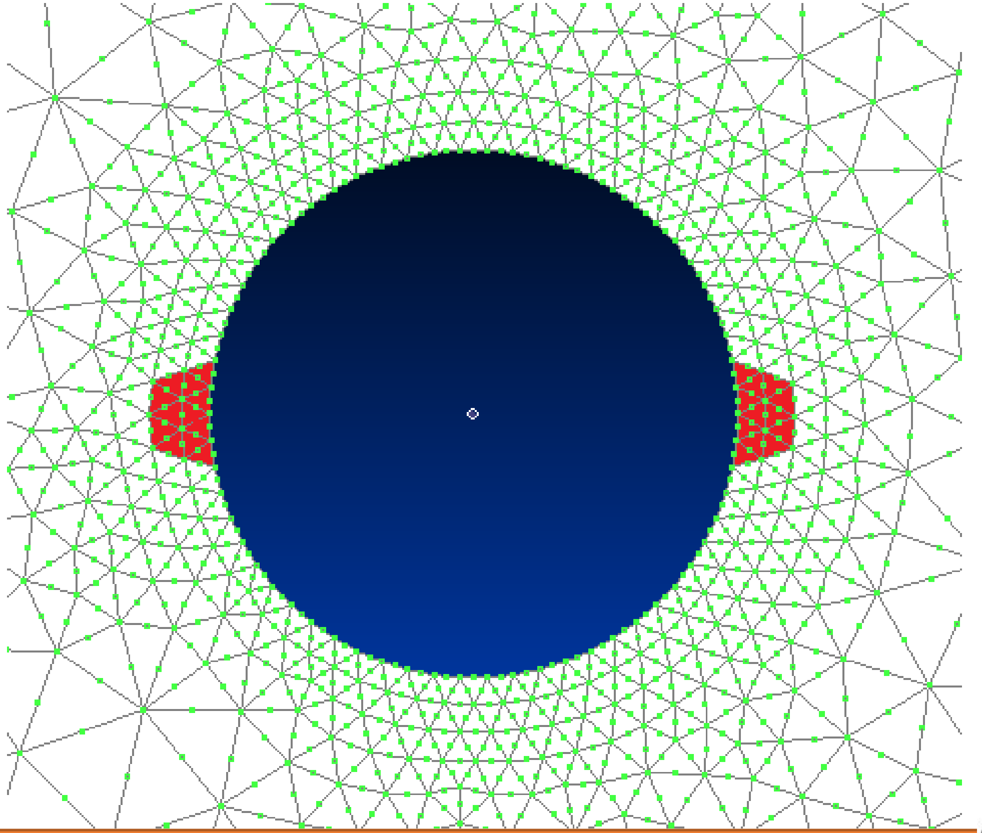

Evaluation of mechanical parameters

- Geomechanical characterization: mostly from laboratory tests on samples from well cores
- Scale of sample and formation are significantly different:

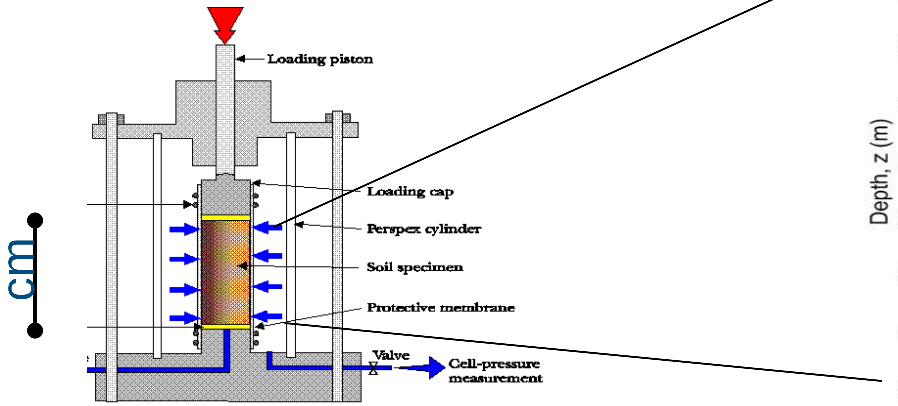

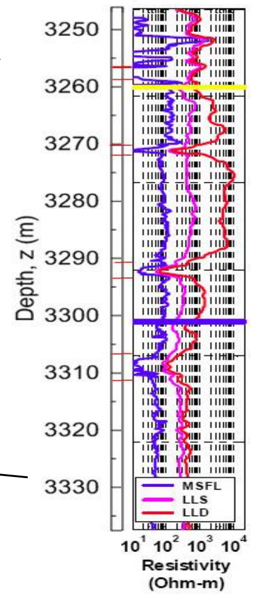

- Need for defining the representativeness of the sample with respect to the problem scale
- Need for evaluating the impact of damage possibly induced by coring

Structure of samples vs structure of geomaterial in situ:

Calcareous rock – photo

Calcareous rock –
x- ray tomography

Sandstone - photo

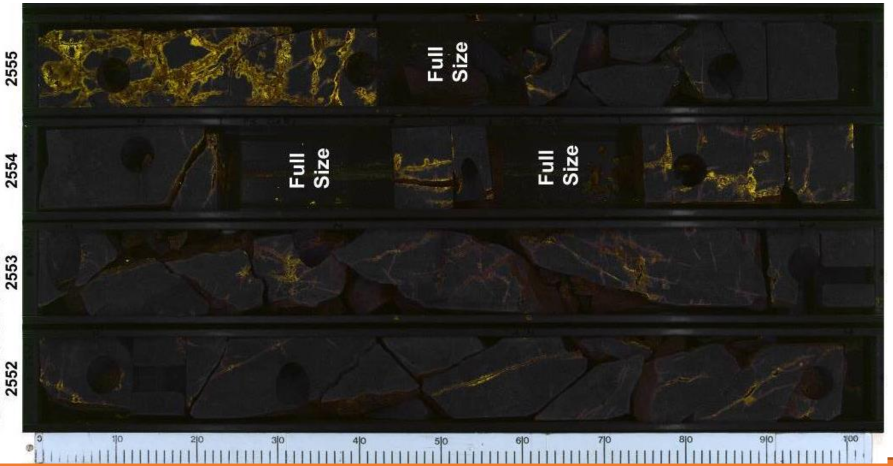

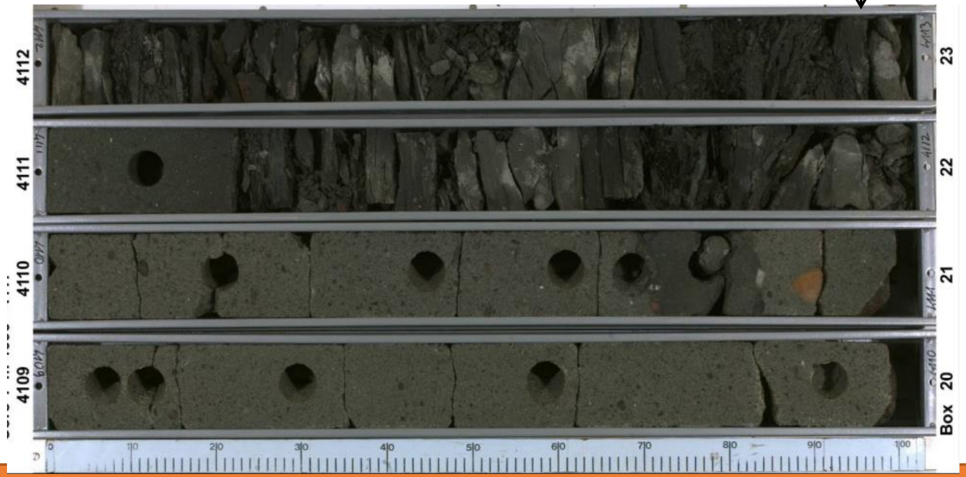

Evaluation of mechanical parameters

Holt M., Brignoli M., Kenter C.J. (2000) Core quality: quantification of coring-induced rock alteration Int. J. of Rock Mechanics and Mining Sciences 37 (2000) 889-907

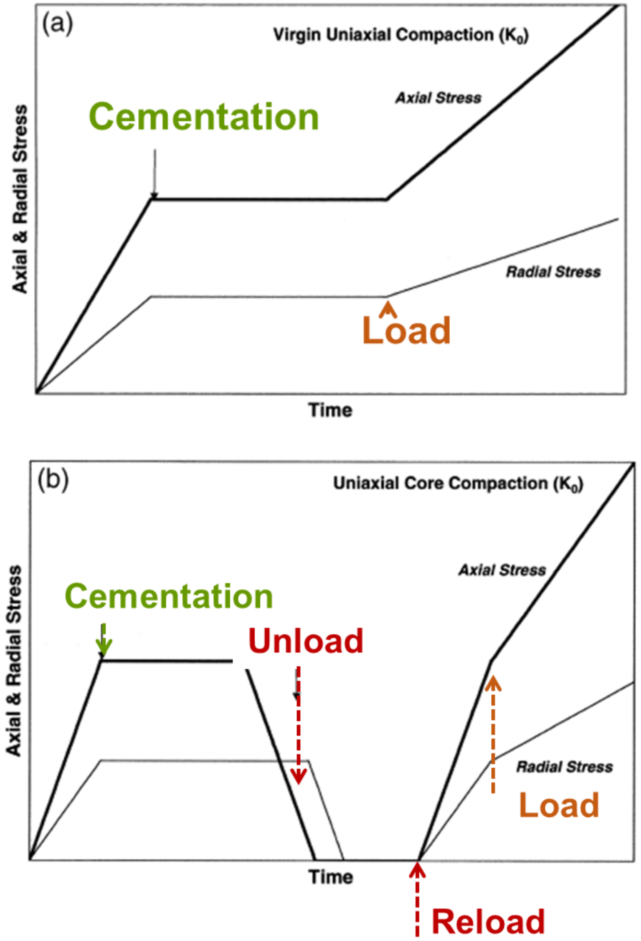

‘virgin’ sample

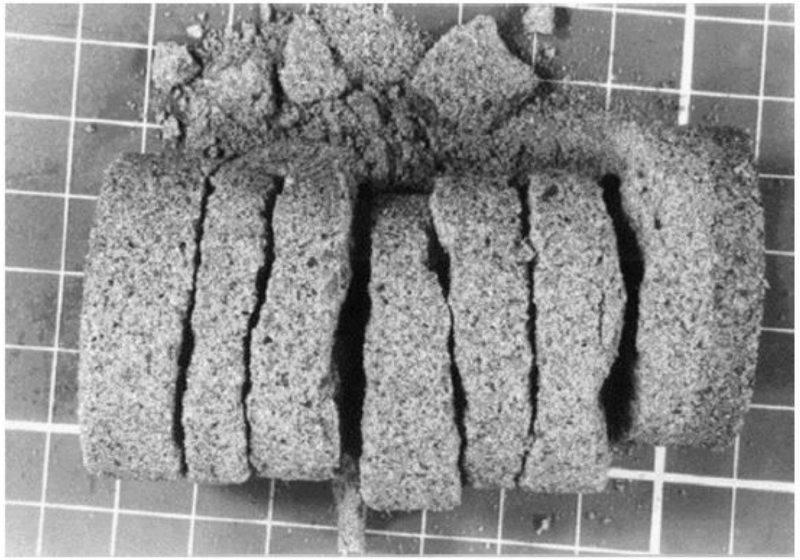

‘cored’ sample

Evaluation of mechanical parameters

Holt M., Brignoli M., Kenter C.J. (2000) *Core quality: quantification of coring-induced rock alteration* Int. J. of Rock Mech. and Min. Sci. 37 (2000) 889-907

‘Virgin’ sample

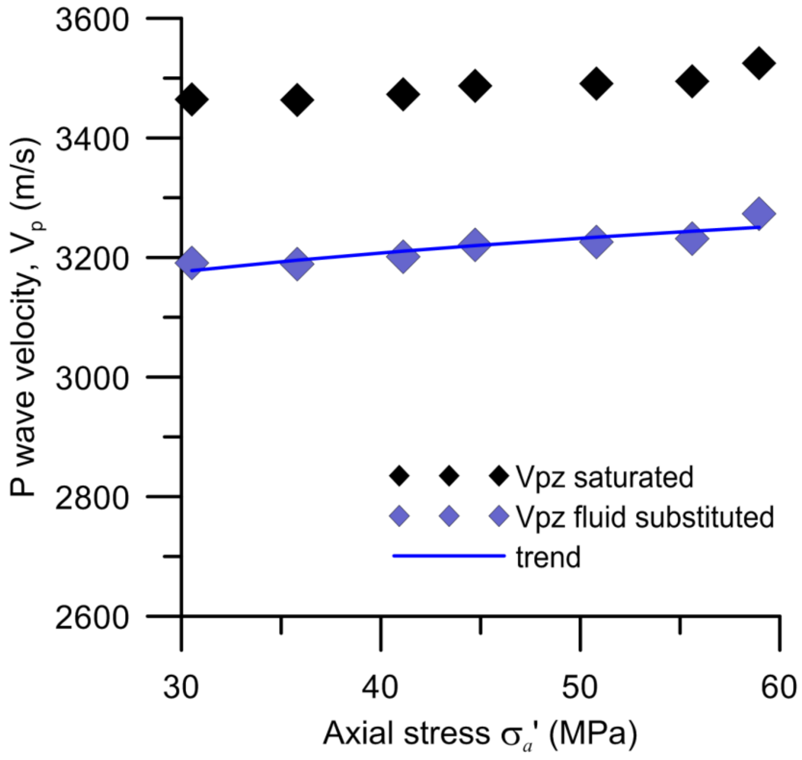

Faster - Relatively independent on stress

‘Cored’ sample

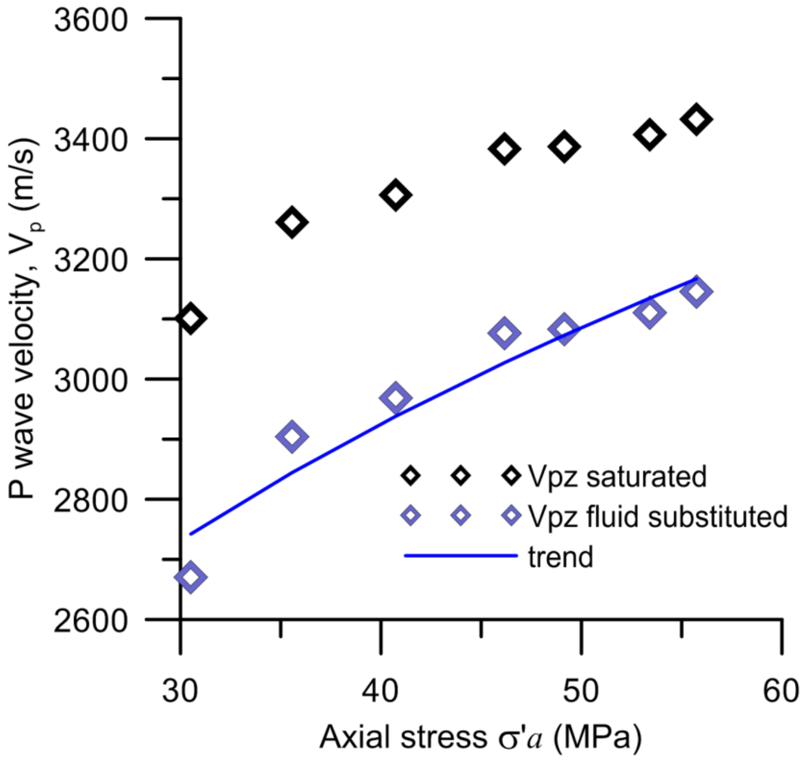

Slower - Moderately dependent on stress

Evaluation of mechanical parameters

Dependency of wave velocity on stress and fabric (related to Hertz –Mindlin theory, (*))

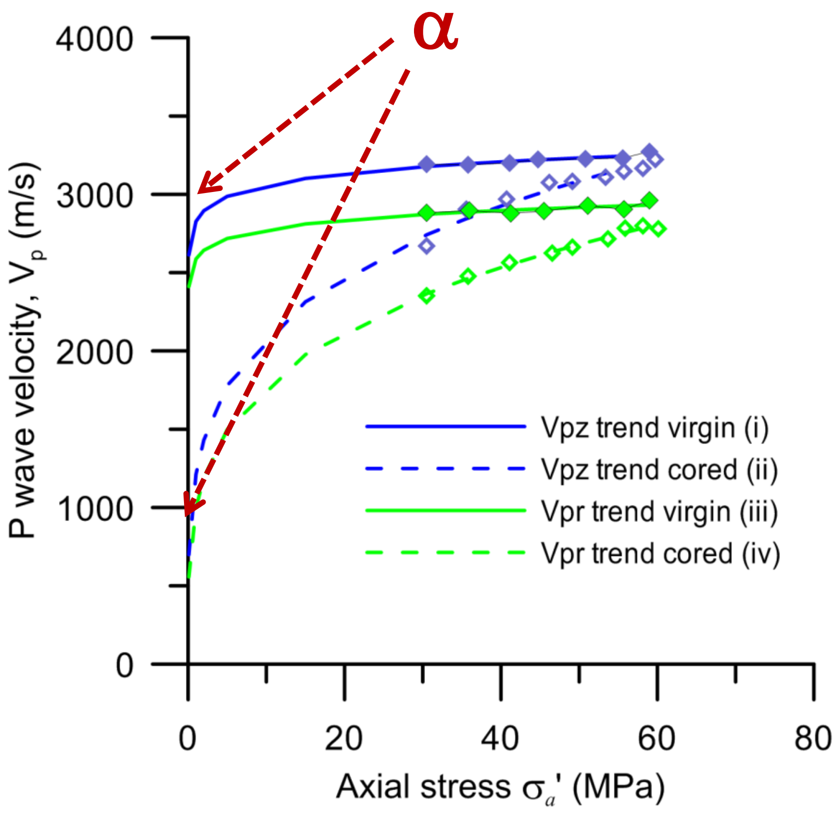

$$V_{P,S} = \alpha_{P,S} \left(\frac{p'}{p_0'} \right)^{\beta_{P,S}}$$

(i) α = 2613 m/s β =0.034

(ii) α = 698.88 m/s β =0.239

$\alpha_{virgin} > \alpha_{cored}$

$\beta_{virgin} < \beta_{cored}$

(*) e.g. Santamarina & Fam (1997), Houlsby & Wroth (1991) ; Viggiani & Atkinson (1995)

Evaluation of mechanical parameters

For idealized assemblies of spherical grains Hertz Mindlin theory
(e.g. Makse et al. 2005)

$$V_p = \frac{1}{\sqrt{\rho}}\left(\frac{3k_n}{20\pi}+\frac{2k_t}{45\pi}\right)^{1/2}\left((1-\phi)Z\right)^{1/3}\left(\frac{6\pi p}{k_n}\right)^{1/6}$$

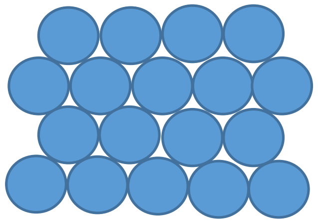

$$V_s = \frac{1}{\sqrt{\rho}}\left(\frac{k_n+2/3k_t}{20\pi}\right)^{1/2}\left((1-\phi)Z\right)^{1/3}\left(\frac{6\pi p}{k_n}\right)^{1/6}$$

P = pressure
Z = average coordination number
(number of contacts per grain)
ϕ = porosity

solid properties | fabric | pressure dependence

α

$\alpha = AF(\phi)$

Heuristic expression for real geomaterials

$V = \alpha\ (p'/p'_0)^{\beta}$

Contact theory versus crack closure theory

Stress dependency of the elastic waves can be expressed also in terms of crack closure (e.g. Katsuki et al., 2013)

Normal and shear stiffness of the cracks (stress dependent)

$$k_n = k_{ni}\left(\frac{\sigma'_n}{\sigma'_{ni}}\right)^n \qquad k_s = k_{si} + k_{sn}\left(\frac{\sigma'_n}{\sigma'_{ni}} - 1\right)$$

In oedometer conditions,

$$V_p = V_{pm}\sqrt{\frac{f_n(p'_{nor})}{1+ f_n(p'_{nor})}} \qquad f_n(p'_{nor}) = \frac{2}{1+K_0} \cdot \frac{s \cdot k_{ni} p'^{n}_{nor}}{M_m} \qquad V_{pm} = \sqrt{M_m/\rho}$$

$$V_s = V_{sm}\sqrt{\frac{f_s(p'_{nor})}{1+ f_s(p'_{nor})}} \qquad f_n(p'_{nor}) = \frac{s \cdot [k_{si} + k_{sn}(p'_{nor} - 1)]}{G_m}$$

V_m - wave velocity of the rock mineral, M_m - modulus of the mineral, s – average spacing

Evaluation of mechanical parameters

Contact theory versus crack closure theory

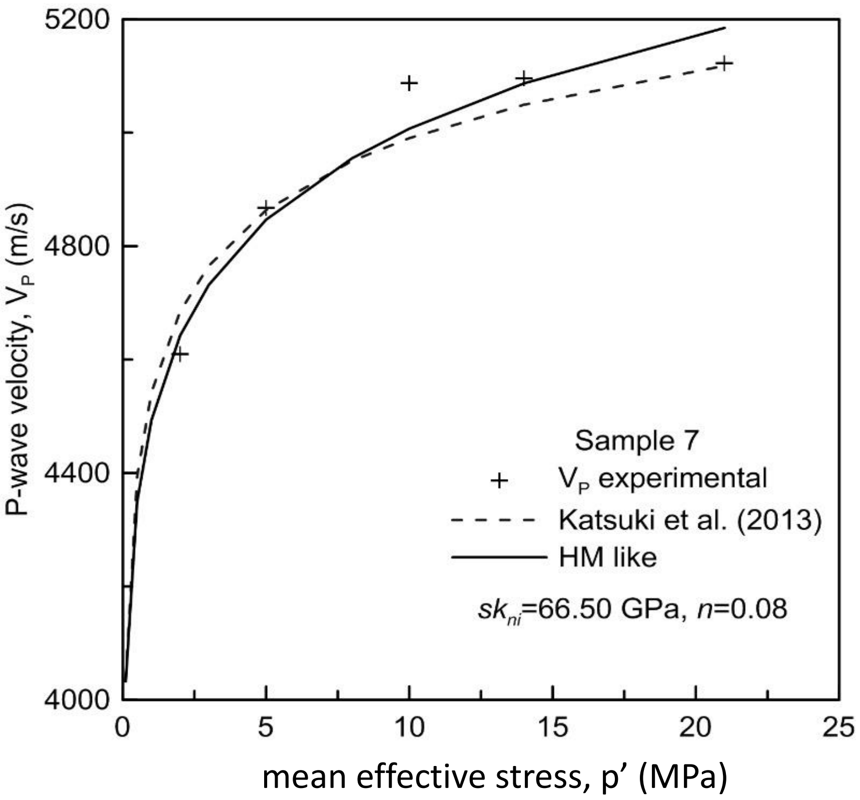

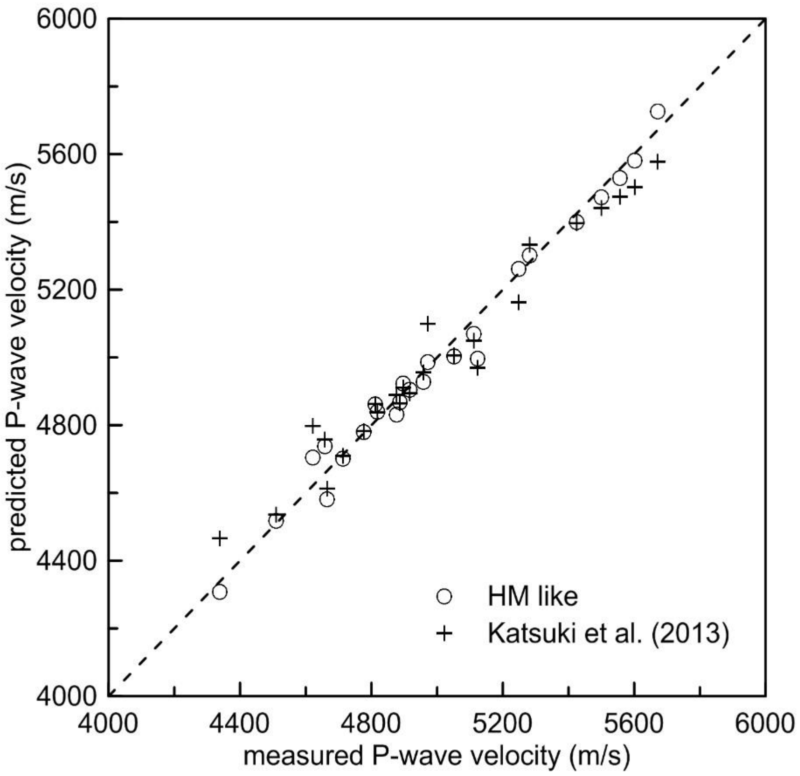

Evaluation of mechanical parameters

Cha, Cho and Santamarina (2009) Long-wavelength P-wave and S-wave propagation in jointed rock masses, Geophysics

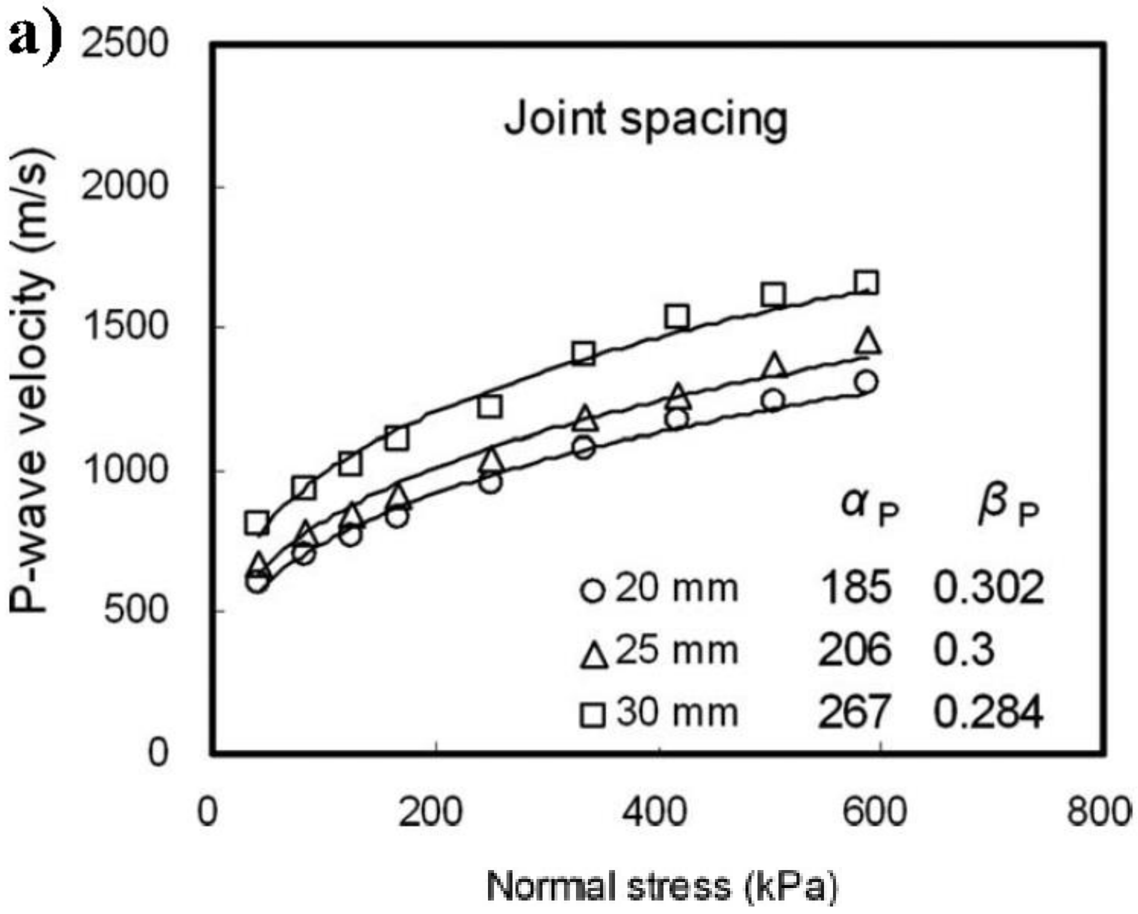

$\alpha_{HS} > \alpha_{SS}$

$\beta_{HS} < \beta_{SS}$

HS Highly Spaced

SS Small Spaced

Cha et al. (2014)

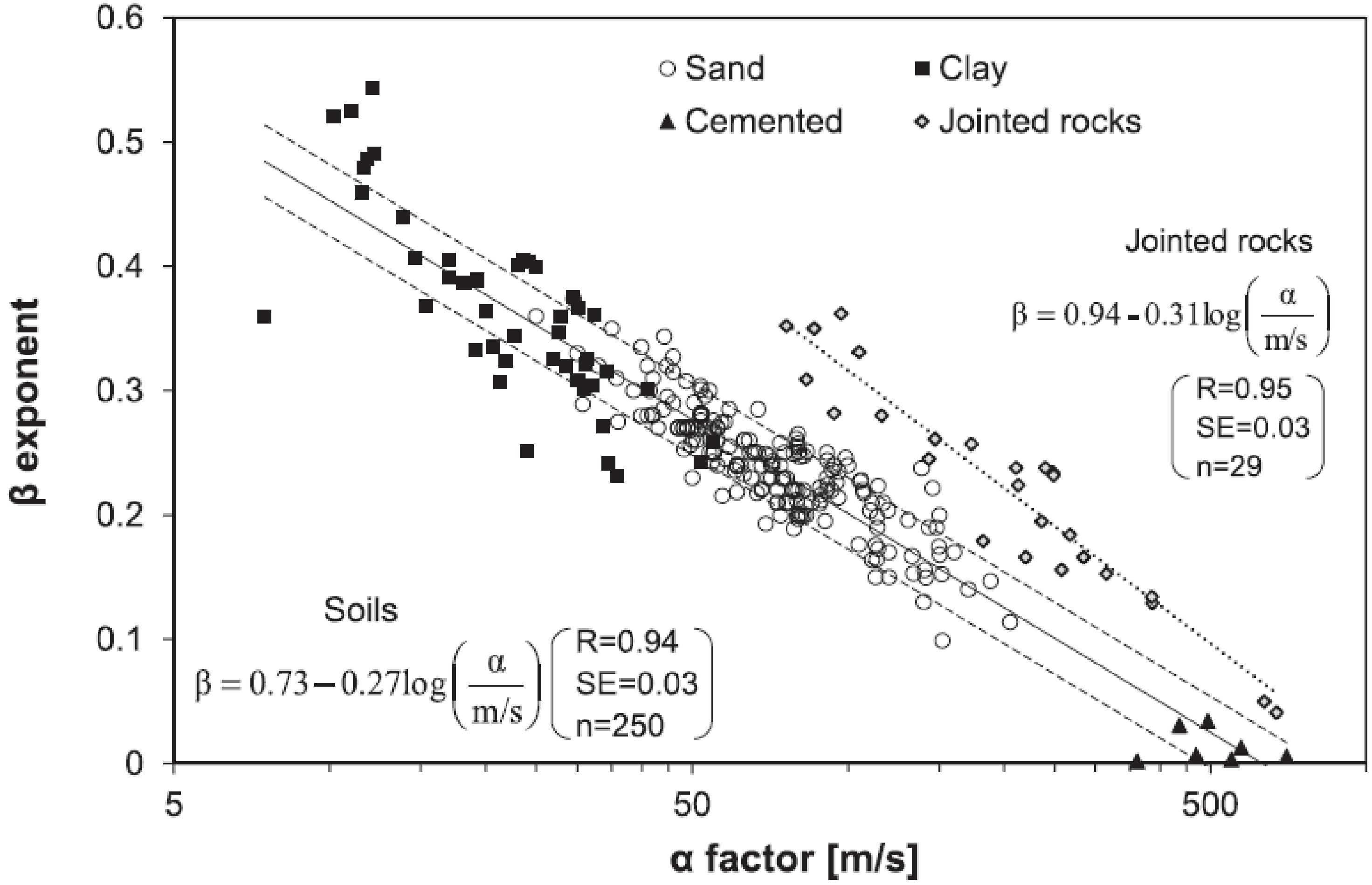

Evaluation of mechanical parameters

Musso, Cosentini, Foti, Comina, Capasso – *Geophysics (2015)*

Lab characterization –structure effects

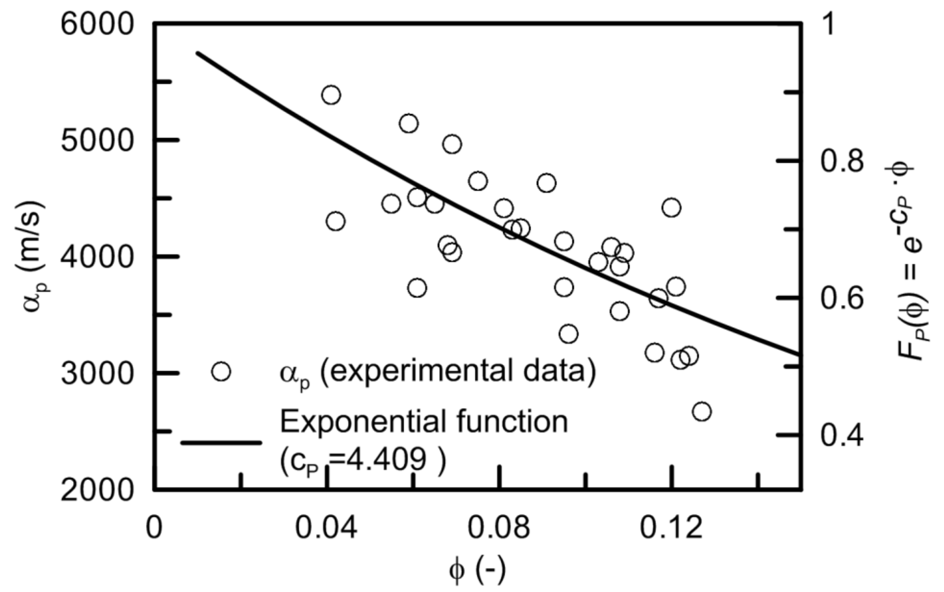

$$\alpha = A\, F(\phi)$$

$$F(\phi) = e^{-c \cdot \phi}$$

$$\alpha = A \cdot e^{-c\phi}$$

A elastic wave velocity in the solid phase

c structural parameter – to be determined through analysis of a mineralogically homogeneous sample dataset from a given reservoir

Scales of investigation

Equipment for laboratory ultrasonic measurements

$f \simeq MHz$

$$\lambda = \frac{V}{f}$$

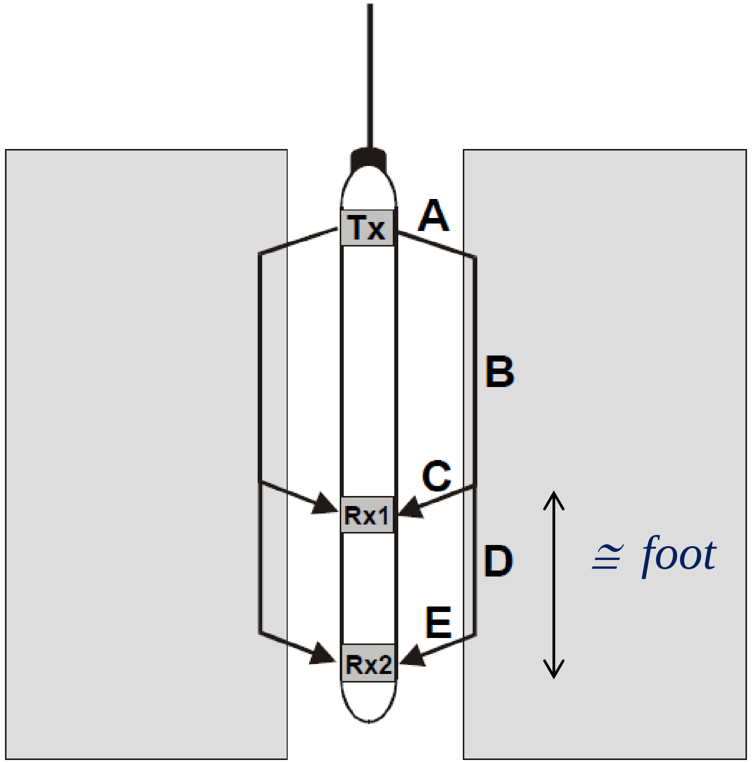

Jointed rock investigated as an equivalent continuum when λ greater than 8-10 s (s – joint spacing) (Cha et al. 2009)

$f \simeq tens\ of\ KHz$

Depth of lateral investigation $\lambda < D < 3\lambda$

α values based on laboratory characterization can be compared with α values deduced from well log measurements

		laboratory	well log
	frequency	ultrasonic (> 30 kHz)	sonic (10 Hz < f < 10 kHz)
(1)	saturation state	imposed	natural
(2)	stress state	imposed	reconstructed
	porosity	measured (directly)	measured (indirectly - logging)
	scale of investigation	sample size (10^{-2} m)	receivers space (m or tens of m)
	effects on structure	coring damage	joints

This is possible provided that:

(1) - reference is made to the same saturation condition (fluid substitution can be applied);

(2) - the stress state in the well is known

Fluid substitution

According to Biot Gassmann theory, provided that frequency is lower than characteristic:

$$f < f_c = \frac{\phi \cdot \eta}{2 \cdot \pi \cdot \rho_{fl} \cdot k}$$

ϕ: porosity;
η: viscosity
ρ_{fl} fluid density
k : permeability

the following relationship holds:

$$K_{sk} = \frac{\left(\frac{\phi}{K_{fl}} + \frac{1-\phi}{K_g}\right) \cdot K_{mix} - 1}{\frac{\phi}{K_{fl}} - \frac{1+\phi}{K_g} + \frac{K_{mix}}{K_g^2}}$$

K_{fl}, K_g, K_{mix}, K_{sk}:
volumetric stiffness of fluid, grain, mixture, skeleton

Example from a carbonatic reservoir

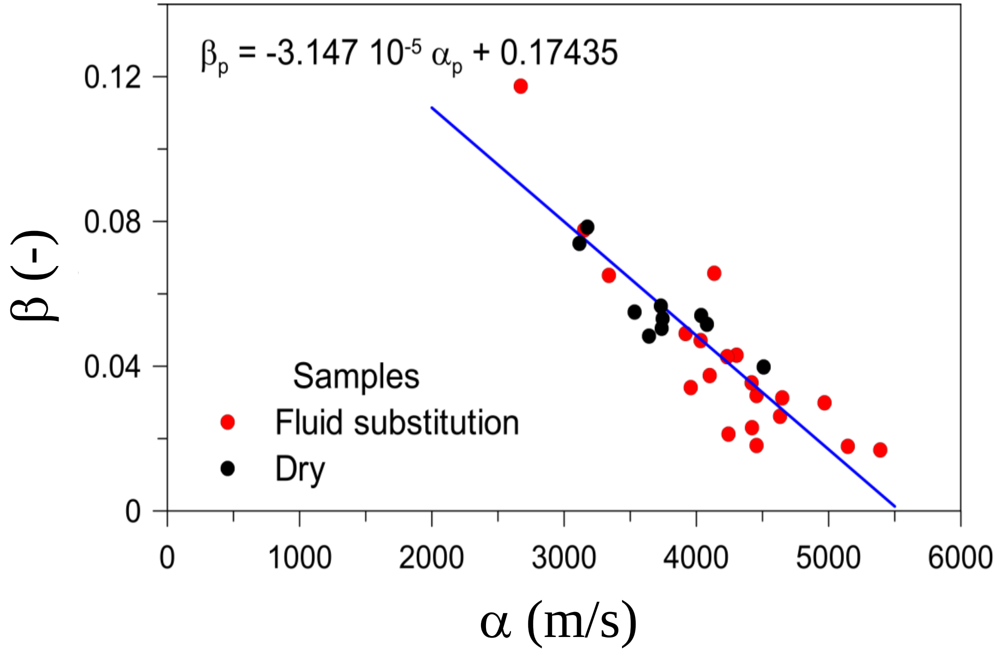

α – β relationship

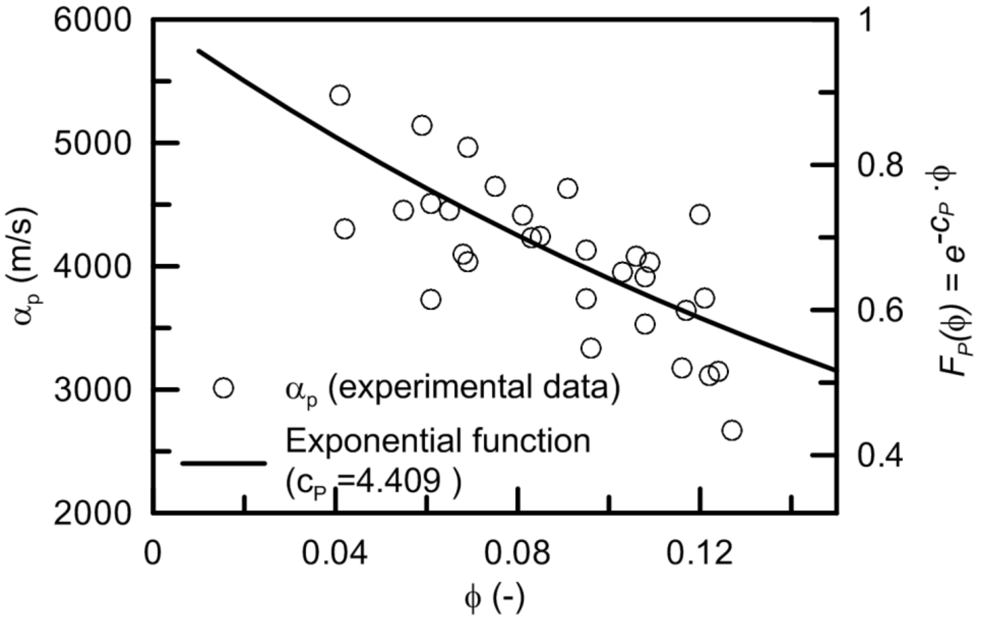

α (or F) – ϕ relationship

Example from a carbonatic reservoir

Step 1: on basis of the *F(ϕ)* from analysis of lab data and porosity log, the profile of expected α along the well is obtained [α^{pseudo}]

$\alpha_p^{pseudo}(\phi)$ $\qquad$ $A_p * F(\phi) = A_p * \exp(-\mathbf{c} * \phi)$

DEPTH (m)	ϕ (-)	Vp F(ϕ)	α_p (ϕ) (m/s)
4014.22	0.114	0.604	3785
4014.98	0.119	0.592	3708
4015.74	0.106	0.628	3934
4016.50	0.094	0.660	4135
4017.26	0.059	0.770	4824
4018.03	0.038	0.844	5288
4018.79	0.047	0.814	5099
4019.55	0.0910	0.670	4196

Example from a carbonatic reservoir

$$SI(z) = \alpha^{well}(z) / \alpha^{pseudo}(\phi)$$

Step 2:

the best estimates of $\alpha^{well}(z)$ (and $\beta^{well}(z)$) are obtained as the couple of values that predicts the measured velocity

DEPTH	$\alpha_p(\phi)$	p'	V_p dry	α_p well	SI
(m)	(m/s)	(Mpa)	(m/s)	(m/s)	(-)
4014.22	3785	11.52	5472	3610	0.954
4014.98	3708	11.52	5302	3768	1.016
4015.74	3934	11.53	5183	4656	1.184
4016.5	4135	11.53	4991	4000	0.967
4017.26	4824	11.53	5621		
4018.03	5288	11.53	5722		
4018.79	5099	11.53	5253		
4019.55	4196	11.53	5253		

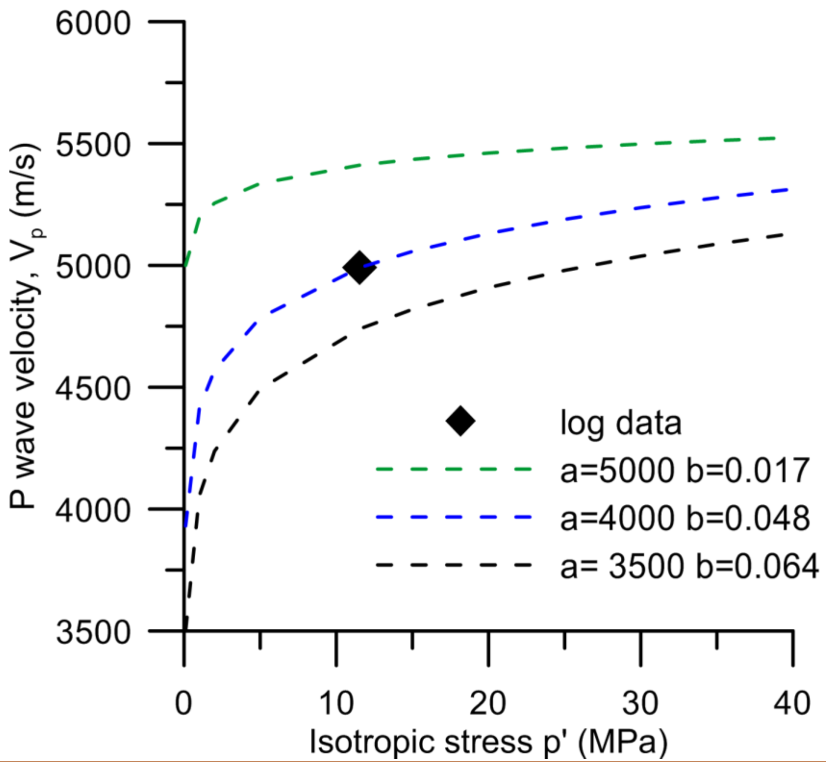

Example from a carbonatic reservoir

SI is low where resistivity is low

(associated to local damaged /weaker zones)

Grochau, M.H. and B. Gurevich, 2008, Investigation of core data reliability to support time-lapse interpretation in Campos Basin, Brazil: Geophysics, **73**, 2: E59-E65.

Grochau, M. and B. Gurevich, 2009, Testing Gassmann fluid substitution: sonic logs versus ultrasonic core measurements: Geophysical Prospecting, **57**, 75-79.

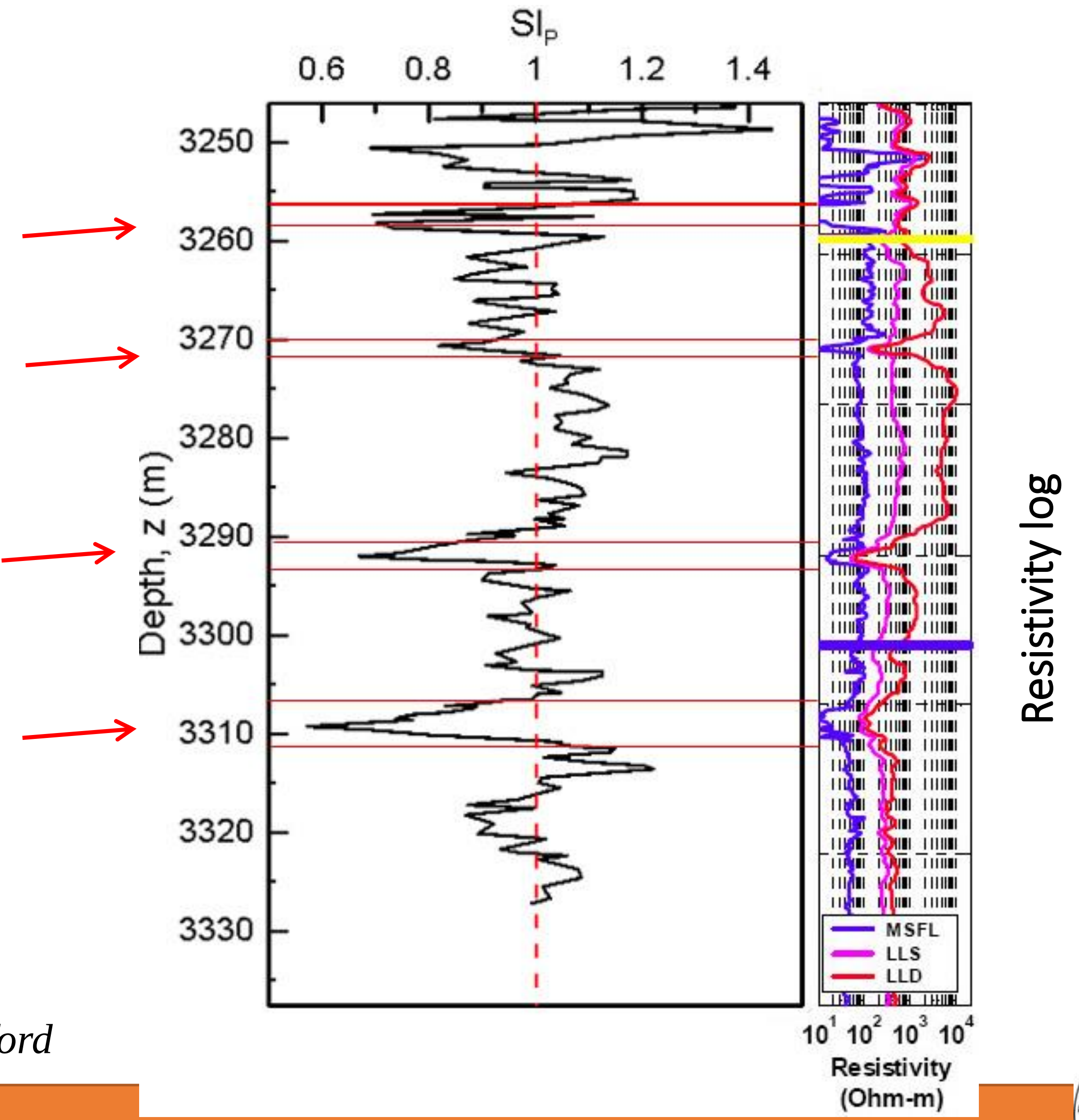

Colombia (Apiay-Guatiquía oil field)

Data from Mantilla (2002) Ph. D. thesis, Stanford

Evaluation of mechanical parameters

Kashagan – well KE5 – structural indexes

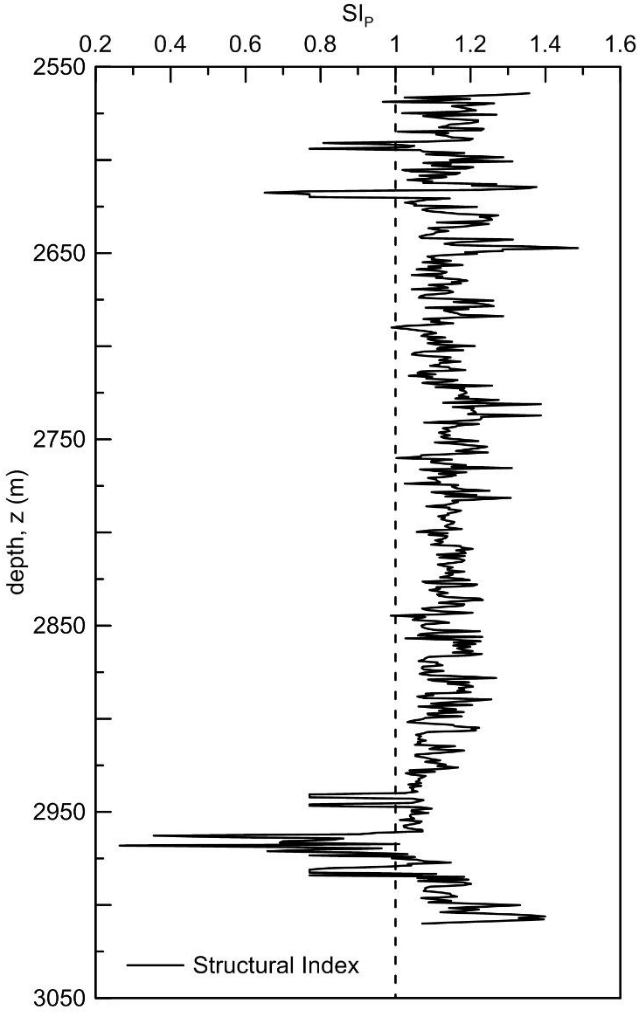

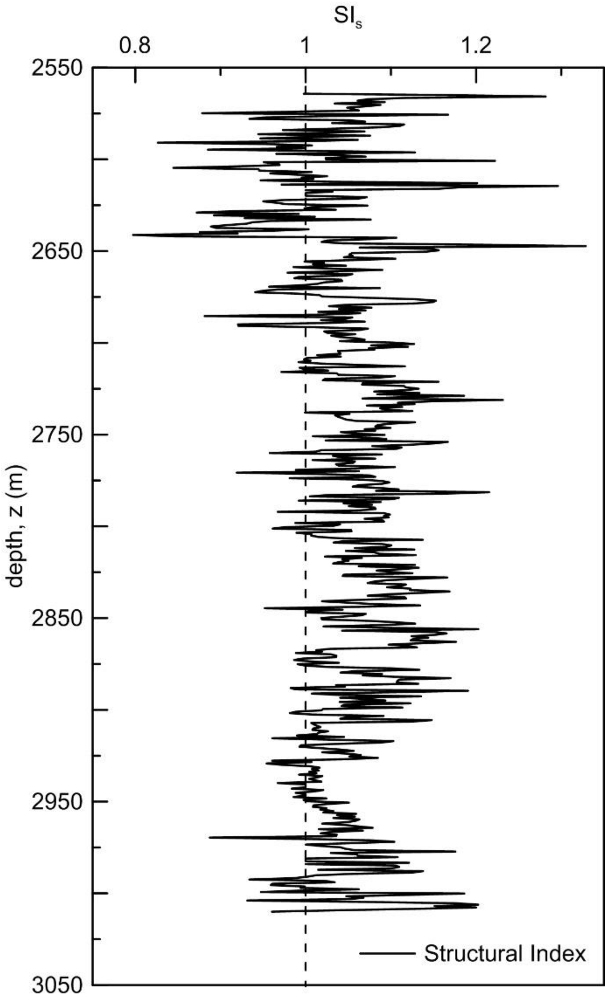

Application to a case study

Capasso, Mantica and Musso. Long-term stability study of open-hole completions in a producing hydrocarbon field. *ARMA 08-238 (San Fransisco)*

HD model (Eclipse)

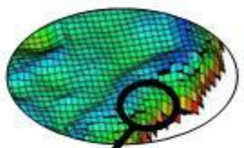

- Load history (pore pressure from HD model) attribution
- Stress-strain evolution

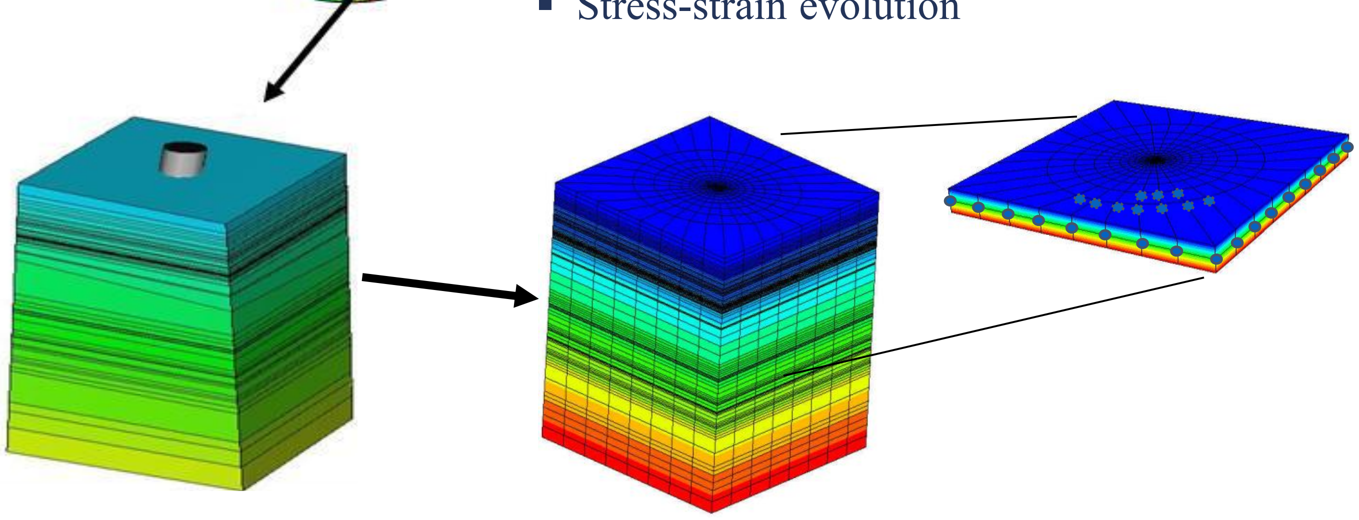

HD model:cell geometry at well location

FE (Abaqus™) model at well location

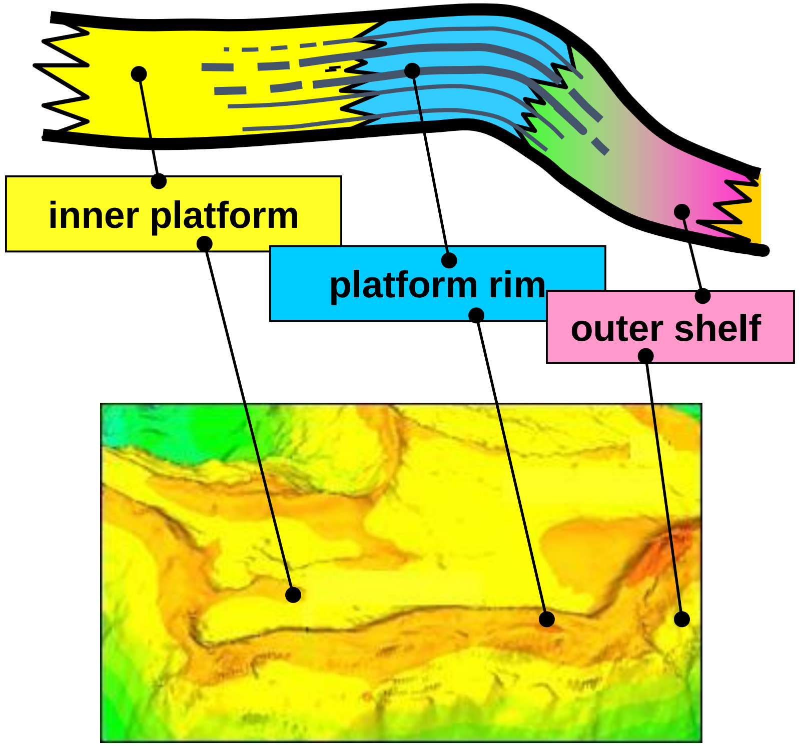

Application to a case study

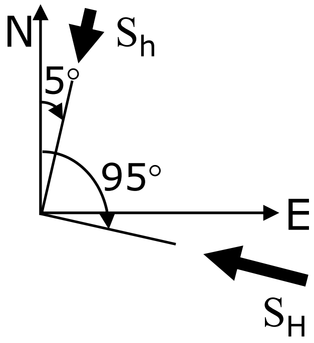

azimuth / deviation	0°	5°N	50°N	95°N
0°	X			
15°		X	X	X
30°		X	X	X

Production history

Load history from Hydro-Dynamic simulation; a logarithmic pressure distribution is determined and applied at each time step according to discharge and steady state conditions

Drilling history

Removal of elements and application of mud pressure on the borehole wall

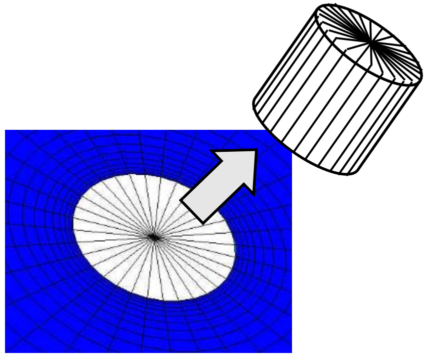

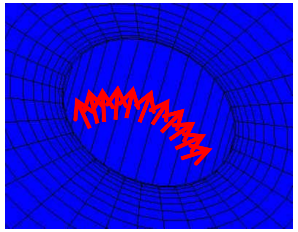

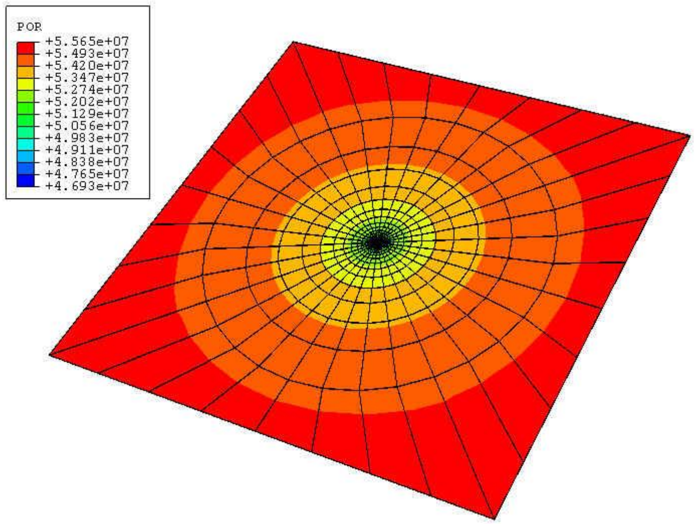

Application to a case study

Deviation 30° - Azimuth 95° (S_H direction)

Plastic deviatoric strain ε_s^{pl} (%)

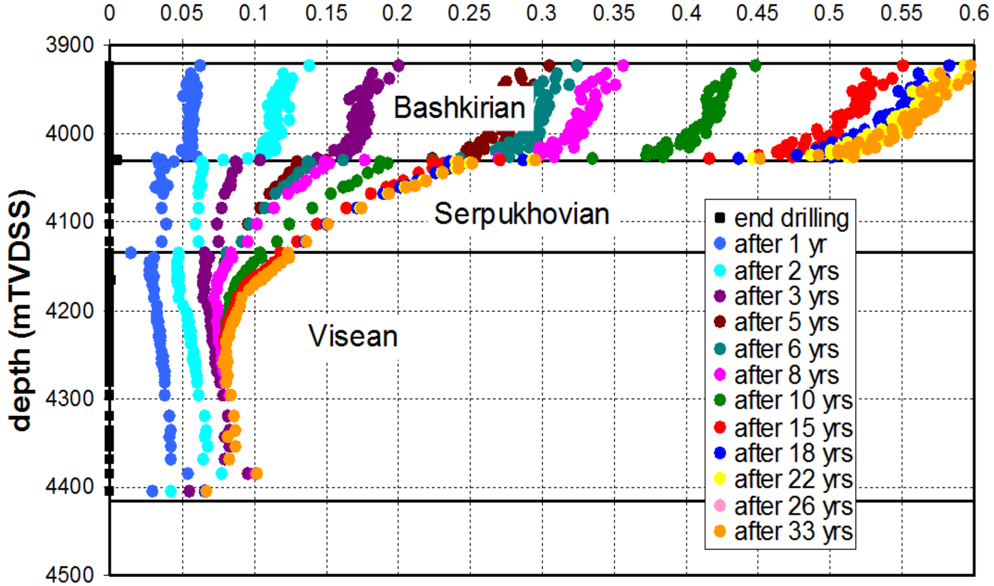

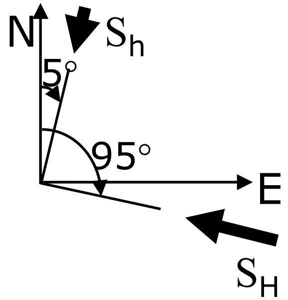

Deviation 30° - Azimuth 5° (S_h direction)

Plastic deviatoric strain ε_s^{pl} (%)

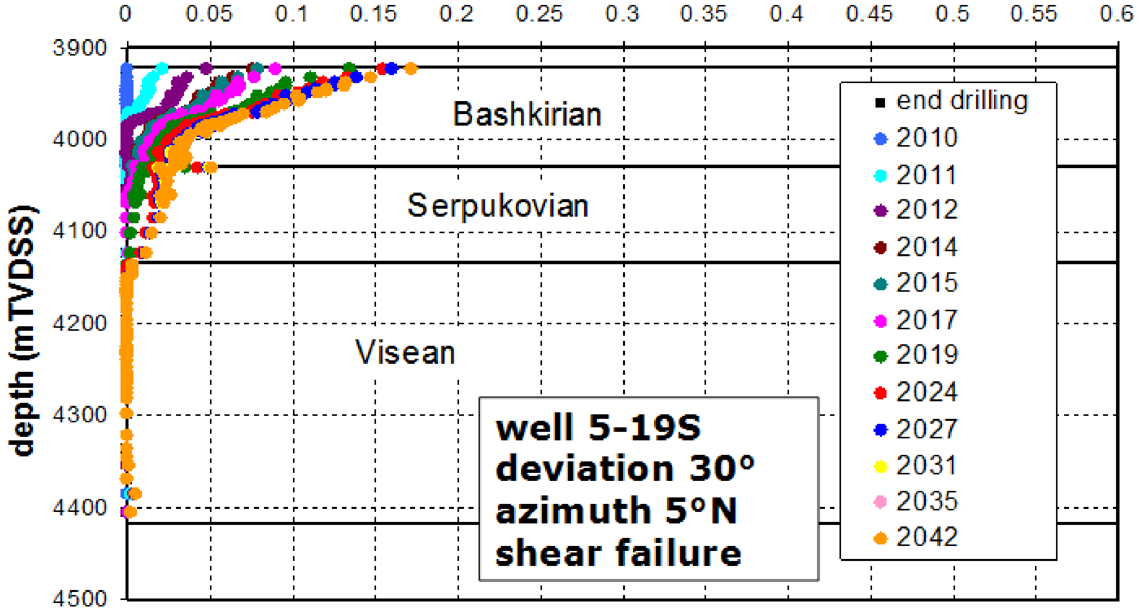

ε_s^{pl} at max shear stress location

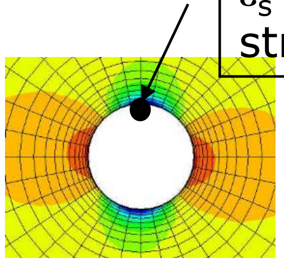

Table of time of failures (*)

deviation	azimuth	failure mode	UNIT 1	UNIT 2	UNIT 3
0°	vertical	Tensile	after 10 yrs	after 10 yrs	drilling
		Shear	after 1 yr	after 1 yr	after 10 yrs
15°	5°N	Tensile	after 8 yrs	after 8 yrs	drilling
		Shear	after 1 yr	after 2 yrs	no failure
	50°N	Tensile	after 8 yrs	after 10 yrs	drilling
		Shear	after 1 yr	after 2 yrs	after 8 yrs
	95°N	Tensile	after 10 yrs	after 18 yrs	drilling
		Shear	after 1 yr	after 2 yrs	after 2 yrs
30°	5°N	Tensile	after 3 yrs	after 3 yrs	drilling
		Shear	after 2 yrs	after 10 yrs	no failure
	50°N	Tensile	after 8 yrs	after 8 yrs	drilling
		Shear	after 1 yr	after 2 yrs	after 8 yrs
	95°N	Tensile	no failure	no failure	drilling
		Shear	start-up	start-up	start-up

(*) Failure assumed to be relevant for ε_s^{pl} 0.04%

Acknowledgments

Gabriele Della Vecchia (Politecnico di Milano)
Anna Pandolfi (Politecnico di Milano)
Gaia Capasso (ENI E&P)
Renato M. Cosentini (Università di Pavia)
Sebastiano Foti (Politecnico di Torino)
Cesare Comina (Università di Torino)